

## ARTICLE



# A blend of broadly-reactive and pathogen-selected V $\gamma$ 4 V $\delta$ 1 T cell receptors confer broad bacterial reactivity of resident memory $\gamma\delta$ T cells

Camille Khairallah<sup>1</sup>, Julie A. Bettke<sup>1</sup>, Oleksandr Gorbatshevych<sup>1</sup>, Zhijuan Qiu<sup>1</sup>, Yue Zhang<sup>1</sup>, Kyungjin Cho<sup>2,3</sup>, Kwang Soon Kim<sup>2,3</sup>, Timothy H. Chu<sup>1</sup>, Jessica N. Imperato<sup>1</sup>, Shinya Hatano<sup>4</sup>, Galina Romanov<sup>1</sup>, Yasunobo Yoshikai<sup>4</sup>, Lynn Puddington<sup>5</sup>, Charles D. Surh<sup>2,3</sup>, James B. Bliska<sup>6</sup>, Adrianus W. M. van der Velden<sup>1</sup> and Brian S. Sheridan<sup>1</sup>✉

© The Author(s), under exclusive licence to Society for Mucosal Immunology 2021

Although murine  $\gamma\delta$  T cells are largely considered innate immune cells, they have recently been reported to form long-lived memory populations. Much remains unknown about the biology and specificity of memory  $\gamma\delta$  T cells. Here, we interrogated intestinal memory V $\gamma$ 4 V $\delta$ 1 T cells generated after foodborne *Listeria monocytogenes* (*Lm*) infection to uncover an unanticipated complexity in the specificity of these cells. Deep TCR sequencing revealed that a subset of non-canonical V $\delta$ 1 clones are selected by *Lm* infection, consistent with antigen-specific clonal expansion. Ex vivo stimulations and in vivo heterologous challenge infections with diverse pathogenic bacteria revealed that *Lm*-elicited memory V $\gamma$ 4 V $\delta$ 1 T cells are broadly reactive. The V $\gamma$ 4 V $\delta$ 1 T cell recall response to *Lm*, *Salmonella enterica* serovar Typhimurium (STm) and *Citrobacter rodentium* was largely mediated by the  $\gamma\delta$ TCR as internalizing the  $\gamma\delta$ TCR prevented T cell expansion. Both broadly-reactive canonical and pathogen-selected non-canonical V $\delta$ 1 clones contributed to memory responses to *Lm* and STm. Interestingly, some non-canonical  $\gamma\delta$  T cell clones selected by *Lm* infection also responded after STm infection, suggesting some level of cross-reactivity. These findings underscore the promiscuous nature of memory  $\gamma\delta$  T cells and suggest that pathogen-elicited memory  $\gamma\delta$  T cells are potential targets for broad-spectrum anti-infective vaccines.

*Mucosal Immunology* (2022) 15:176–187; <https://doi.org/10.1038/s41385-021-00447-x>

## INTRODUCTION

Mucosal tissues are critical interfaces with the environment for the maintenance of the body's integrity. These barriers are constantly exposed to a wide range of stresses that need local immune monitoring to promote health. As such, mucosa resident leukocytes are crucial patrolling sentinels that must eliminate invading pathogens while maintaining a beneficial relationship with harmless commensal microorganisms and other innocuous antigens<sup>1,2</sup>.  $\gamma\delta$  T cells are unconventional lymphocytes ideally located within these barrier tissues where they provide a multitude of functions<sup>3</sup>. In mice, most mucosal resident  $\gamma\delta$  T cells harbor invariant or semi-invariant (pairing of an invariant and a variable chain) T cell receptors (TCR)<sup>4</sup> and are thought to respond in a TCR independent, preprogrammed fashion to cytokines or pathogen products in the periphery<sup>5,6</sup>. In humans, the thymus supports the development of semi-invariant type 1 and type 3  $\gamma\delta$  T cell subsets with innate-like transcriptomic signatures that persist into adulthood<sup>7</sup>. Because of these features, these  $\gamma\delta$  T cell subsets are commonly seen as innate-like cells.

Although immunological memory has largely been defined in the context of conventional antigen-specific  $\alpha\beta$  T cells and B cells, the recent identification of unconventional memory responses has expanded this view<sup>8</sup>. Several studies have demonstrated that murine  $\gamma\delta$  T cells can mount long-lasting memory responses, extending the observations made more than a decade ago in non-human primate infection models<sup>9</sup>. Using a mouse-adapted *Listeria monocytogenes* (*Lm*) strain<sup>10</sup>, we previously showed that food-borne infection of mice generates a multifunctional resident memory  $\gamma\delta$  T cell population in the intestines and draining mesenteric lymph nodes (MLN) that is maintained in the absence of antigenic stimulation<sup>11</sup>. This population is characterized by a CD44<sup>hi</sup> CD27<sup>ne9</sup> phenotype and the expression of a semi-invariant V $\gamma$ 4 V $\delta$ 1 TCR (nomenclature<sup>12</sup>), consisting of an invariant, canonical V $\gamma$ 4 chain associated with a more diverse V $\delta$ 1 chain. Upon secondary exposure, memory  $\gamma\delta$  T cells collaborate with conventional T cells to provide optimal protection by orchestrating the formation of organized granulomatous structures that restrain *Lm* growth in the MLN through IL-17A production<sup>11,13</sup>. Memory  $\gamma\delta$  T cell responses were subsequently reported in response to other

<sup>1</sup>Department of Microbiology and Immunology, Center for Infectious Diseases, Renaissance School of Medicine, Stony Brook University, Stony Brook, NY, USA. <sup>2</sup>Academy of Immunology and Microbiology, Institute for Basic Science, Pohang, Republic of Korea. <sup>3</sup>Division of integrative Biosciences & Biotechnology, Pohang University of Science and Technology, Pohang, Republic of Korea. <sup>4</sup>Division of Immunology and Genome Biology, Medical Institute of Bioregulation, Kyushu University, Fukuoka, Japan. <sup>5</sup>Department of Immunology, University of Connecticut Health, Farmington, CT, USA. <sup>6</sup>Department of Microbiology and Immunology, Geisel School of Medicine at Dartmouth, Dartmouth College, Hanover, NH, USA. ✉email: [brian.sheridan@stonybrook.edu](mailto:brian.sheridan@stonybrook.edu)

Received: 7 March 2021 Revised: 3 August 2021 Accepted: 16 August 2021

Published online: 30 August 2021

bacterial infections<sup>14–16</sup> and imiquimod-induced skin inflammation<sup>17,18</sup>. Surprisingly, several of these memory responses mobilized innate-like  $\gamma\delta$  T cells expressing semi-invariant TCR, suggesting that the role of these cells is more complex than originally proposed.

$\gamma\delta$  T cell specificity remains mostly elusive. Nevertheless, these lymphocytes respond to a large variety of host-derived and microbial antigens that are by nature distinct from  $\alpha\beta$  T cells<sup>19</sup>. The antigen reactivity of the different memory  $\gamma\delta$  T cell subsets reported so far remains unknown. The ligand of the canonical V $\gamma$ 4 V $\delta$ 1 TCR is expressed or presented by peritoneal macrophages and upregulated after intraperitoneal (i.p.) *Lm* infection, providing evidence of a conserved host-derived antigen consistent with the semi-restricted TCR repertoire of this  $\gamma\delta$  T cell subset<sup>20</sup>. However, we previously showed that *Lm*-elicited V $\gamma$ 4 V $\delta$ 1 memory T cells do not respond to foodborne *Salmonella enterica* serovar Typhimurium (STm) infection, indicating contextual specificity to *Lm*<sup>11</sup>. Similarly, *Bordetella pertussis* (*Bp*)-induced V $\gamma$ 2 memory T cells demonstrated some level of specificity to *Bp*<sup>15</sup>, suggesting that the ligands recognized by these two memory  $\gamma\delta$  T cell subsets may be of bacterial origin. These observations suggest that memory  $\gamma\delta$  T cells could be selected by both host-derived and bacterial antigens. In line with this, the V $\gamma$ 4 V $\delta$ 1 T cell population elicited by foodborne *Lm* infection comprises both canonical and non-canonical subpopulations that may have distinct specificities and could be differentially selected by host-derived and microbial antigens during infection. However, it remains undefined whether exposure to *Lm* induces the clonal expansion and selection of V $\gamma$ 4 V $\delta$ 1 T cells that is commonly associated with antigen recognition and indicative of T cell specificity.

The tight association of *Lm*-elicited memory  $\gamma\delta$  T cells with the gastrointestinal system and their semi-invariant TCR suggest a broad role in immunosurveillance at this major entry point for pathogens. Thus, the reactivity of these adaptive  $\gamma\delta$  T cells was evaluated in response to the foodborne pathogens *Lm*, *Yersinia pseudotuberculosis* (*Yp*), and *Citrobacter rodentium* (*Cr*) and the murine model of STm-induced colitis. These pathogens represent a broad group of bacteria with diverse replicative life cycles. Instead of a tightly restricted specificity, our data revealed a broad TCR-mediated reactivity of *Lm*-elicited memory V $\gamma$ 4 V $\delta$ 1 T cells against pathogenic bacteria that is driven by a combination of clones expressing canonical and non-canonical V $\delta$ 1 TCRs. Although the majority of the response was carried out by cells expressing canonical TCRs, a substantial proportion of non-canonical clones were expanded upon *Lm* or STm infection, indicating that some form of selection occurs after infection. Interestingly, a very small number of non-canonical clones appeared to cross-react against both *Lm* and STm-induced colitis infections, contributing to both responses. Collectively, these findings reveal degrees of adaptive  $\gamma\delta$  T cell specificity and broad-spectrum reactivity that may provide new cellular targets for anti-infective vaccines.

## RESULTS

### Involvement of the TCR in $\gamma\delta$ T cell responses to foodborne *Lm* infection

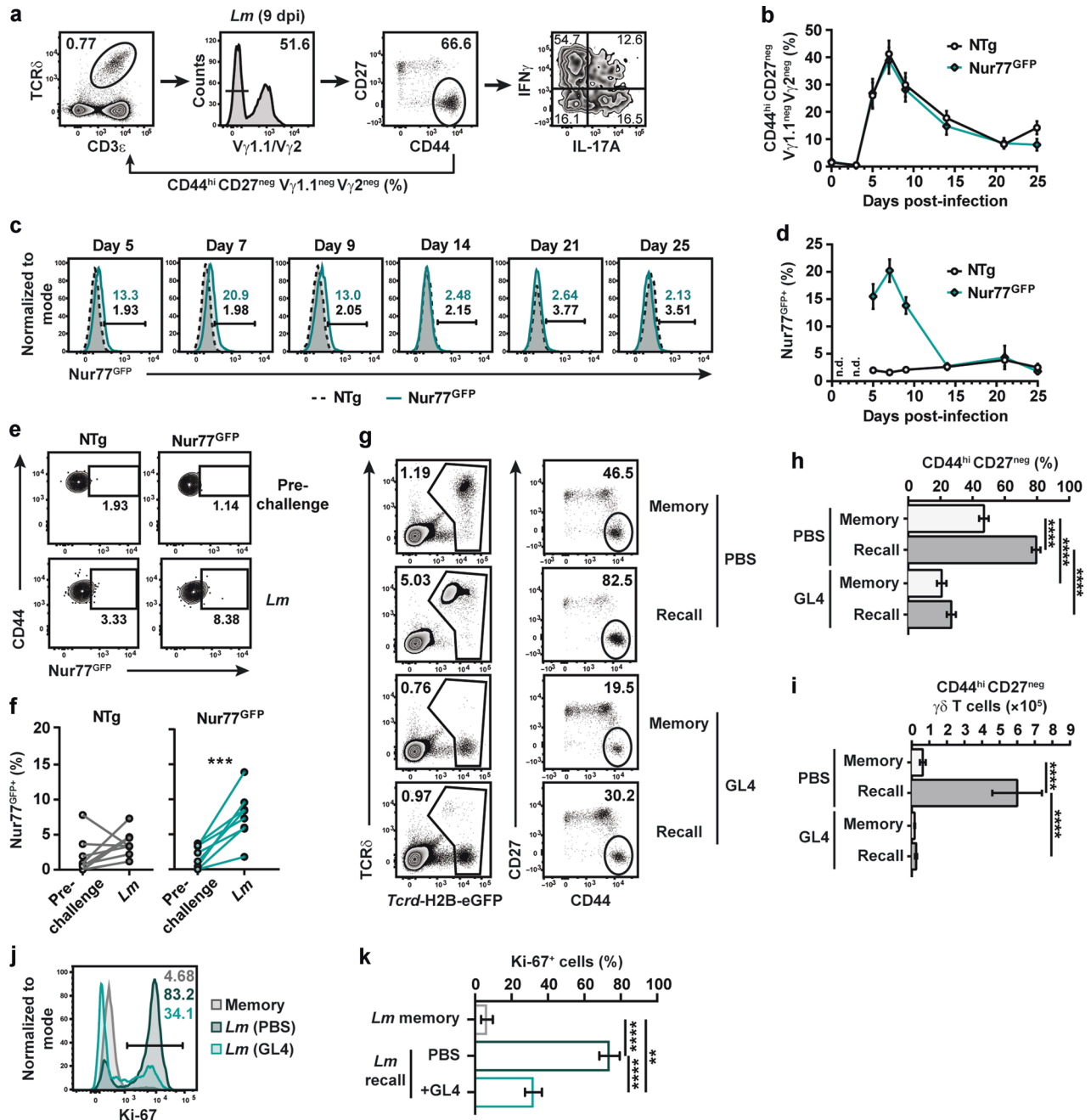
The protection provided by memory  $\gamma\delta$  T cells upon secondary *Lm* exposure relies on surface expression of the  $\gamma\delta$ TCR<sup>11</sup>, suggesting that TCR signaling is required for the recall of memory  $\gamma\delta$  T cells. To assess whether TCR signaling was elicited during the immune response to foodborne *Lm* infection, a longitudinal analysis of circulating  $\gamma\delta$  T cells was performed in Nur77<sup>GFP</sup> and control non-transgenic (NTg) mice. Nur77<sup>GFP</sup> reporter mice are commonly used to assess TCR signaling in T cells as Nur77 is an orphan nuclear receptor that is upregulated upon TCR-mediated activation<sup>21</sup>. Of note, *Lm*-elicited  $\gamma\delta$  T cells are generated and similarly multi-functional in both Balb/c and C57Bl/6 mice after foodborne *Lm*

infection (ref. <sup>11</sup> and unpublished data). Consistent with our previous observations, *Lm*-elicited  $\gamma\delta$  T cells (identified as CD44<sup>hi</sup> CD27<sup>neg</sup> V $\gamma$ 1.1<sup>neg</sup> V $\gamma$ 2<sup>neg</sup>, see Fig. 1a) were mobilized into the blood as early as 5 days after infection, peaked around day 7 and contracted thereafter (Fig. 1b). A significant fraction of cells was GFP<sup>+</sup> from 5 to 9 days post-infection (dpi) and GFP expression rapidly vanished during contraction (Fig. 1c, d). *Lm* challenge infection of *Lm*-immune Nur77<sup>GFP</sup> mice also resulted in an increase of GFP<sup>+</sup> cell frequency in the blood 4 days after secondary infection (Fig. 1e, f). To assess TCR mediated induction of Nur77<sup>GFP</sup> expression, we stimulated MLN single-cell suspensions from *Lm*-immune Nur77<sup>GFP</sup> and NTg mice with anti-CD3 $\epsilon$  and anti-CD28 or anti-TCR $\delta$  (clone GL4) antibodies and compared the expression of Nur77<sup>GFP</sup> in conventional and unconventional T cells. Nur77<sup>GFP</sup> expression was robustly upregulated in activated CD44<sup>hi</sup> CD4<sup>+</sup> and CD8<sup>+</sup> T cells (Fig. S1a–c). TCR engagement on CD44<sup>hi</sup> CD27<sup>neg</sup>  $\gamma\delta$  T cells led to TCR internalization and Nur77<sup>GFP</sup> expression, albeit to a lesser degree than conventional T cells (Fig. S1d–g). Hence, TCR signaling was engaged in *Lm*-elicited  $\gamma\delta$  T cells during both effector phases of the immune response to *Lm*.

We next evaluated whether expression of the  $\gamma\delta$ TCR regulates the recall response to foodborne *Lm* infection in  $\gamma\delta$  T cell reporter *Tcrd*-H2B-eGFP mice<sup>22</sup>.  $\gamma\delta$  T cells in these mice constitutively express GFP and are identifiable in absence of surface expression of the  $\gamma\delta$ TCR (Fig. 1g). Treatment of *Lm*-immune *Tcrd*-H2B-eGFP mice with the anti-TCR $\delta$  antibody clone GL4 induces the internalization of the TCR rather than depleting  $\gamma\delta$  T cells (Fig. 1g–i; ref. <sup>11</sup>), although a significant decrease in the frequency of CD44<sup>hi</sup> CD27<sup>neg</sup>  $\gamma\delta$  T cells was noted (Fig. 1h). GL4 treatment abrogated CD44<sup>hi</sup> CD27<sup>neg</sup>  $\gamma\delta$  T cell expansion upon *Lm* challenge (Fig. 1h, i) and significantly inhibited their proliferation, as indicated by the substantial reduction in Ki-67 expression (Fig. 1j, k). Similar results were obtained in mice treated with the UC7-13D5 antibody, which also triggers the internalization of the  $\gamma\delta$ TCR (Fig. S2a; ref. <sup>22</sup>), although the effect was less robust (Fig. S2b–d). Consistent with these observations, TCR internalization did not overtly activate CD44<sup>hi</sup> CD27<sup>neg</sup>  $\gamma\delta$  T cells as IFN $\gamma$  and IL-17A were not induced after GL4 treatment (Fig. S2e, f). Importantly, TCR internalization did not elicit a nonresponsive state as  $\gamma\delta$  T cell function was largely intact in response to TCR-independent stimulation with PMA and ionomycin (Fig. S2g–j). A subtle but significant decrease in IL-17A production was observed with or without stimulation in the GL4-treated group. As *Lm* burden is comparable between infected GL4- and PBS-treated *Lm*-immune mice<sup>11</sup>, this suggests that surface expression of the TCR provides critical signals that mediate anamnestic  $\gamma\delta$  T cell responses.

### Canonical and non-canonical V $\delta$ 1 clones participate in anamnestic responses to *Lm*

The TCR dependency described above suggests that memory  $\gamma\delta$  T cells respond to antigens that are expressed or upregulated during infection. Effector  $\gamma\delta$  T cells elicited by primary *Lm* infection revealed an almost exclusively canonical V $\gamma$ 4 chain but showed some diversity in the V $\delta$ 1 TCR repertoire<sup>11</sup>, suggesting that variations in the CDR3 $\delta$  sequence might influence the cell's specificity and reveal some TCR-mediated selection. However, this previous study relied on traditional approaches that lacked sequencing depth as only 30 V $\delta$ 1 TCR sequences were assessed. Therefore, deep sequencing approaches were used to analyze the repertoire of sort-purified *Lm*-elicited V $\gamma$ 4 V $\delta$ 1 T cells. Since no antibody specific for the V $\gamma$ 4 TCR chain was available until very recently, an indirect strategy to identify V $\gamma$ 4 V $\delta$ 1 T cells for cell sorting and flow cytometry analysis was used (Fig. S3a). Analysis of CDR3 $\gamma$  sequences confirmed that the vast majority of sorted cells expressed TRGV6 transcripts (which encodes V $\gamma$ 4), of which >96% were canonical and consistent with our published observations<sup>11</sup>. Although some of the transcripts recovered represented other TRGV gene segments, particularly TRGV2 (which encodes V $\gamma$ 1.2;



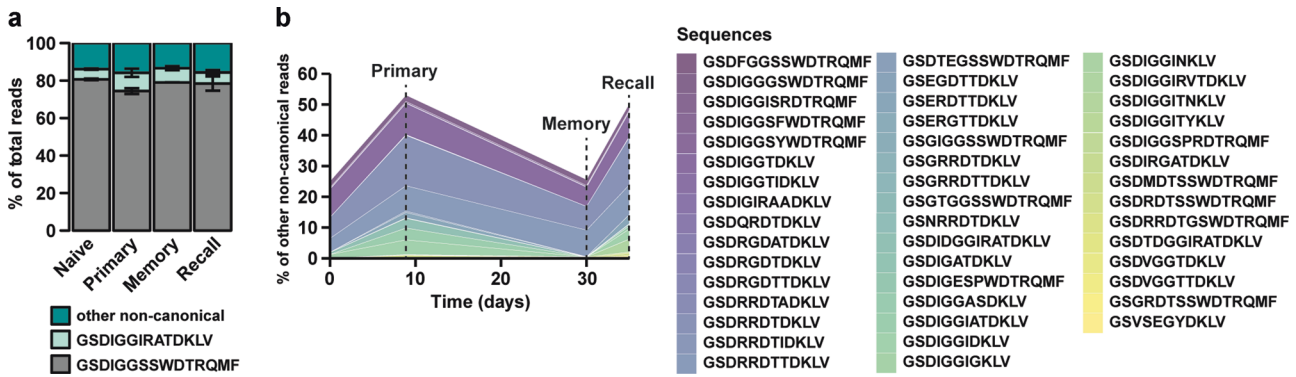


**Fig. 2** Canonical and non-canonical clones contribute to the V $\delta$ 1 T cell recall response to *Lm* challenge infection. CD44<sup>hi</sup> CD27<sup>neg</sup> V $\gamma$ 1.1<sup>neg</sup> V $\gamma$ 2<sup>neg</sup>  $\gamma\delta$  T cells were sort purified from the MLN of mice undergoing a primary, memory or recall response to foodborne *Lm* infection. CD44<sup>hi</sup> CD27<sup>neg</sup> V $\gamma$ 1.1<sup>neg</sup> V $\gamma$ 2<sup>neg</sup>  $\gamma\delta$  T cells were sort purified from the MLN, spleen, and pLN from naive mice. CDR3 $\delta$  transcripts were sequenced and V $\delta$ 1 sequences were selected for further analyses. **a** Percent of total reads mapping to the canonical (gray), public non-canonical (light green), or other non-canonical sequences (dark green), in the naive, primary, memory, and recall samples averaged across two biological samples. **b** Percent of non-canonical reads from two combined biological samples mapping to sequences that are expanded in primary vs naive and recall vs memory conditions. Each color represents an individual clone to aid visualization.

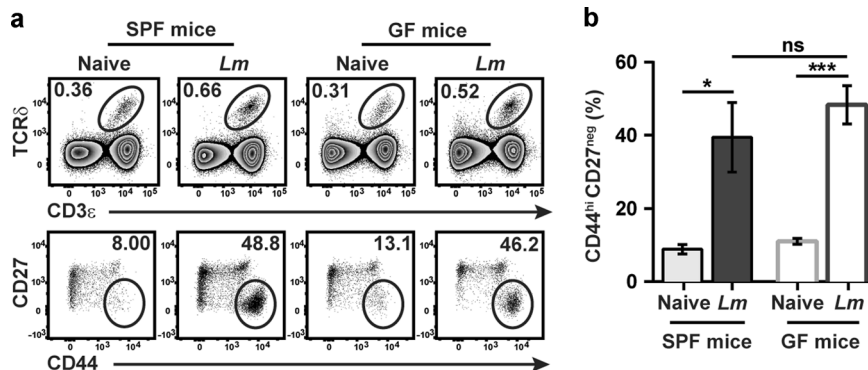


**Fig. 3** Bacterial infection can elicit adaptive  $\gamma\delta$  T cell responses independent of the microbiota. SPF and GF mice were left uninfected or orally infected with *Lm*, and  $\gamma\delta$  T cells were analyzed in the MLN at 9 dpi. **a** Representative dot plots are shown. **b** Cumulative data of the frequency of CD44<sup>hi</sup> CD27<sup>neg</sup>  $\gamma\delta$  T cells among total  $\gamma\delta$  T cells from two independent experiments are shown as mean  $\pm$  SEM ( $n = 3-6$  mice/group/experiment). \* $p < 0.05$ ; \*\*\* $p < 0.001$ .

Fig. S3b), the presence of non-V $\gamma$ 4<sup>+</sup> cells in our sorting strategy was minimal as assessed by flow cytometric analysis using the V $\gamma$ 4-specific 1C10-1F7 antibody<sup>23</sup>. Indeed, virtually all the cells in the sorted gate were positively stained with the 1C10-1F7, but not the V $\gamma$ 1.1/V $\gamma$ 1.2 cross-reactive 4B2.9 antibody (Fig. S3c–e). Thus, this strategy faithfully identified V $\gamma$ 4 T cells.

To assess whether *Lm* infection leads to the selection of specific V $\delta$ 1 clones, CDR3 $\delta$  analysis was performed on two independent biological replicates throughout the different phases of the immune response (naive and *Lm* primary, memory and secondary responses). As expected, the invariant canonical GSDIGGSSWDTRQMF sequence represented most of the repertoire throughout the immune response, followed by the non-canonical public (a rearranged TCR shared among most individuals) GSDIGGIRATDKLV sequence (Fig. 2a). However, a sizeable population did not express either conserved TCRs and will be referred to as “non-canonical” hereafter. Interestingly, a subset of non-canonical clones expanded upon primary infection, contracted at memory and expanded after recall challenge (Fig. 2b), a behavior reminiscent of antigen-specific conventional memory T cells. Similar to the heterogeneity of a polyclonal T cell response, the non-canonical population consisted mostly of infrequent clones but also included abundant clones (<0.5% or between 1.5 and 17% of the non-canonical reads, respectively). These data show that while *Lm* infection expands the canonical and public V $\gamma$ 4 V $\delta$ 1 TCR, it also selects for specific non-canonical

V $\gamma$ 4 V $\delta$ 1 TCR clones, suggesting that the TCR can impart some degree of specificity to adaptive  $\gamma\delta$  T cell responses.

### Microbiota is not necessary for CD44<sup>hi</sup> CD27<sup>neg</sup> $\gamma\delta$ T cell response to *Lm* infection

Since the majority of cells responding to *Lm* expressed the canonical TCR and because the ligand for the canonical V $\gamma$ 4 V $\delta$ 1 TCR appears to be a conserved, host-derived molecule whose expression on macrophages is regulated by infection<sup>20</sup>, we hypothesized that some of the elicited  $\gamma\delta$  T cells might respond to other bacteria. Acute enteric infections can transiently disrupt intestinal barrier integrity, allowing commensals to disseminate extra-intestinally and induce pathogen- as well as commensal-specific conventional T cells<sup>24</sup>. Several reports have shown that subsets of  $\gamma\delta$  T cells can also be differentially modulated by the microbiota, including in the intestines<sup>9,25</sup>. Because *Lm*-elicited adaptive  $\gamma\delta$  T cells share several phenotypic and functional features with commensal-induced  $\gamma\delta$  T cells, we evaluated whether CD44<sup>hi</sup> CD27<sup>neg</sup>  $\gamma\delta$  T cells may be responding to disseminating commensals after oral *Lm* infection. The absence of a microbiota did not appear to impact the development of this subset at steady state as CD44<sup>hi</sup> CD27<sup>neg</sup>  $\gamma\delta$  T cells in the MLN were present at comparably low frequencies in naive specific pathogen-free (SPF) and germ-free (GF) mice (Fig. 3a). After oral *Lm* infection, a similar proportion of CD44<sup>hi</sup> CD27<sup>neg</sup>  $\gamma\delta$  T cells were elicited in the MLN of SPF and GF mice (Fig. 3b),

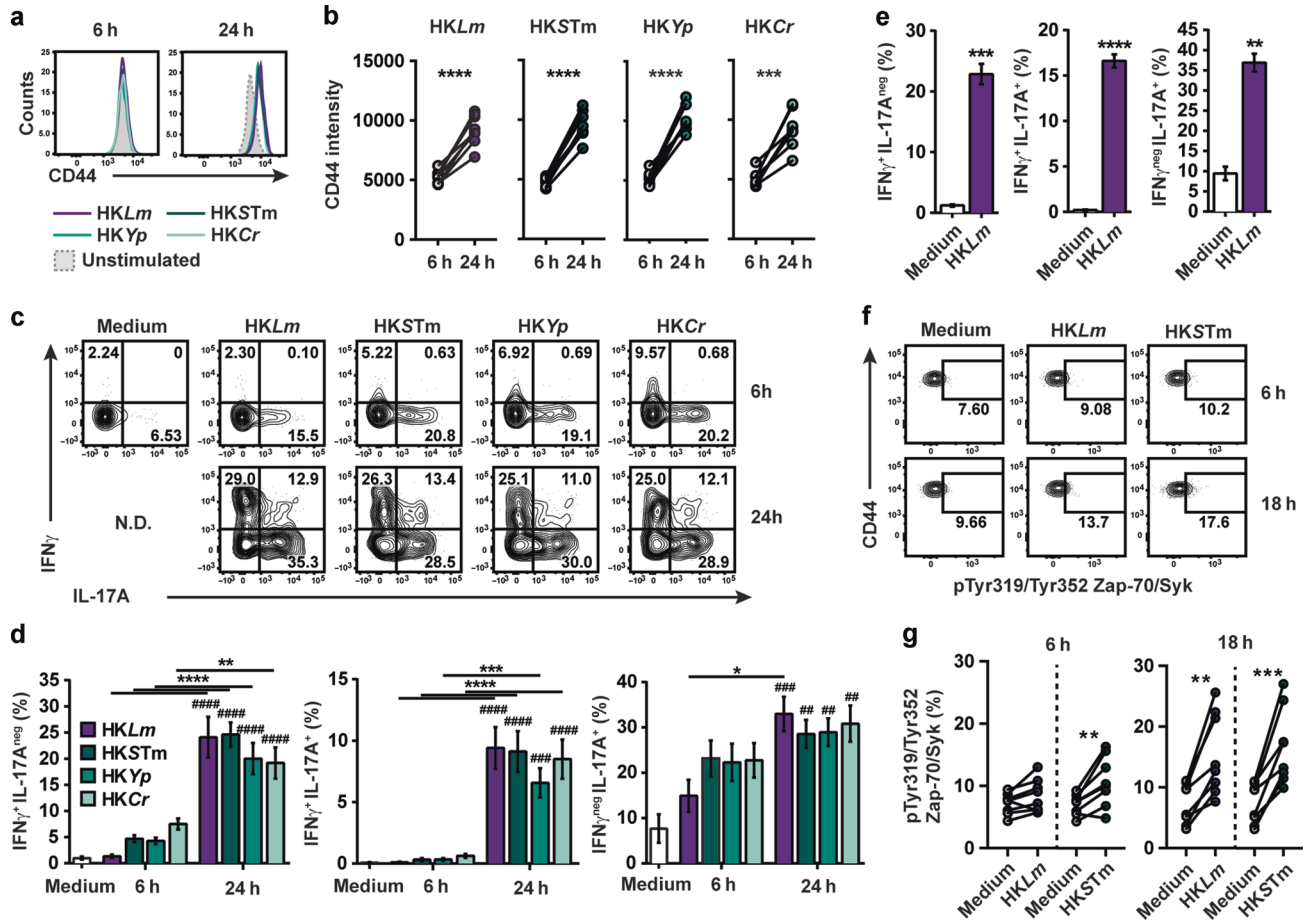


**Fig. 4 Multifunctional response of *Lm*-elicited memory  $\gamma\delta$  T cells to heterologous enteropathogenic bacteria *ex vivo*.** Single-cell suspensions of MLN from *Lm*-immune mice were stimulated for 6, 18, or 24 h with the indicated heat-killed (HK) bacteria (MOI 10) or left unstimulated (medium), and memory CD44<sup>hi</sup> CD27<sup>neg</sup> V $\gamma$ 1.1<sup>neg</sup> V $\gamma$ 2<sup>neg</sup>  $\gamma\delta$  T cells were analyzed. **a** Representative histograms of CD44 expression are shown. **b** Scatter plots show the mean  $\pm$  SEM of CD44 MFI. **c** Representative flow plots of IFN $\gamma$  and IL-17A production are shown. **d** Bar graphs show the mean  $\pm$  SEM percentage of cytokine-producing cells. Significant differences with the unstimulated sample are depicted by # symbols. Differences between stimulated samples are represented by \* symbols. All graphs depict the cumulative data from two independent experiments ( $n = 4$  biological replicates/condition/experiment). **e** Bar graphs show the mean  $\pm$  SEM percentage of cytokine-producing memory CD44<sup>hi</sup> CD27<sup>neg</sup> V $\gamma$ 1.1<sup>neg</sup> V $\gamma$ 2<sup>neg</sup>  $\gamma\delta$  T cells after 24 h-stimulation with HKLm and are representative of two independent experiments. **f** Representative flow plots of pTyr319/Tyr352 Zap-70/Syk expression by memory CD44<sup>hi</sup> CD27<sup>neg</sup> V $\gamma$ 1.1<sup>neg</sup> V $\gamma$ 2<sup>neg</sup>  $\gamma\delta$  T cells after stimulation with the indicated HK bacteria for 6 or 18 h. Gates were based on individual FMO controls. **g** Scatter plots depict the cumulative data of two independent experiments as the mean  $\pm$  SEM percentage of pTyr319/Tyr352 Zap-70/Syk<sup>+</sup> cells among memory CD44<sup>hi</sup> CD27<sup>neg</sup> V $\gamma$ 1.1<sup>neg</sup> V $\gamma$ 2<sup>neg</sup>  $\gamma\delta$  T cells ( $n = 4$  samples/condition/experiment). A paired analysis was performed to determine significant differences between conditions. \* $p \leq 0.05$ ; \*\* and ## $p \leq 0.01$ ; \*\*\* and ### $p \leq 0.001$ ; \*\*\*\* and #### $p \leq 0.0001$ .

demonstrating that the microbiota is not necessary for the induction of a primary adaptive  $\gamma\delta$  T cell response after oral *Lm* infection.

#### Multiple pathogenic bacteria elicit a multifunctional response from memory V $\gamma$ 4 V $\delta$ 1 T cells *ex vivo*

To further assess specificity, the adaptive V $\gamma$ 4 V $\delta$ 1 T cell response to multiple pathogens was evaluated. To this end, bulk MLN cells from *Lm*-immunized mice were stimulated with diverse heat-killed (HK) mouse or human pathogens including *Lm*, *STm*, *Yp*, and *Cr*. CD44<sup>hi</sup> CD27<sup>neg</sup> V $\gamma$ 1.1<sup>neg</sup> V $\gamma$ 2<sup>neg</sup>  $\gamma\delta$  T cells showed a significant increase in CD44 expression with all pathogens between 6 and 24 h of culture (Fig. 4a, b), which was accompanied by a robust and multifunctional effector response involving IFN $\gamma$ <sup>+</sup> producers and IFN $\gamma$ <sup>+</sup>IL-17A<sup>+</sup> coproducers at 24 but not 6 h (Fig. 4c, d). IL-17A<sup>+</sup> single producers were readily detectable at 6 h and further increased at 24 h. These multifunctional responses were not observed at 24 h in the absence of stimulation (Fig. 4e). Interestingly, V $\gamma$ 2<sup>+</sup> T cells also produced IL-17A after 24 h (Fig.

S4a, b), but only memory V $\gamma$ 4 V $\delta$ 1 T cells produced IFN $\gamma$  under these conditions despite the presence of IFN $\gamma$ -biased V $\gamma$ 1.1<sup>+</sup> and CD27<sup>+</sup> V $\gamma$ 4 T cells (Fig. S4c–f). These results demonstrate that *Lm*-elicited memory V $\gamma$ 4 V $\delta$ 1 T cells have the capacity to respond to diverse bacteria.

Given the involvement of the TCR in *Lm*-elicited V $\gamma$ 4 V $\delta$ 1 T cell responses to *Lm* *in vivo* (Fig. 1), we assessed whether TCR signaling was elicited in cultures stimulated with HKLm and HKSTm. Phosphorylation of the TCR proximal tyrosine kinases Zap-70 and Syk was used to identify TCR signaling. Consistent with the minimal cytokine production observed in 6 h cultures, only a slight increase in the phosphorylation of Zap-70/Syk was observed with HKSTm but not HKLm (Fig. 4f, g). However, a significant increase in pZap-70/Syk was detected in both cultures at 18 h, demonstrating that TCR signaling occurred in CD44<sup>hi</sup> CD27<sup>neg</sup> V $\gamma$ 1.1<sup>neg</sup> V $\gamma$ 2<sup>neg</sup>  $\gamma\delta$  T cells in response to HK bacteria. Collectively, these data show that *Lm*-elicited memory V $\gamma$ 4 V $\delta$ 1 T cell contact with diverse enteric bacteria induces TCR signals and results in a delayed multifunctional response.

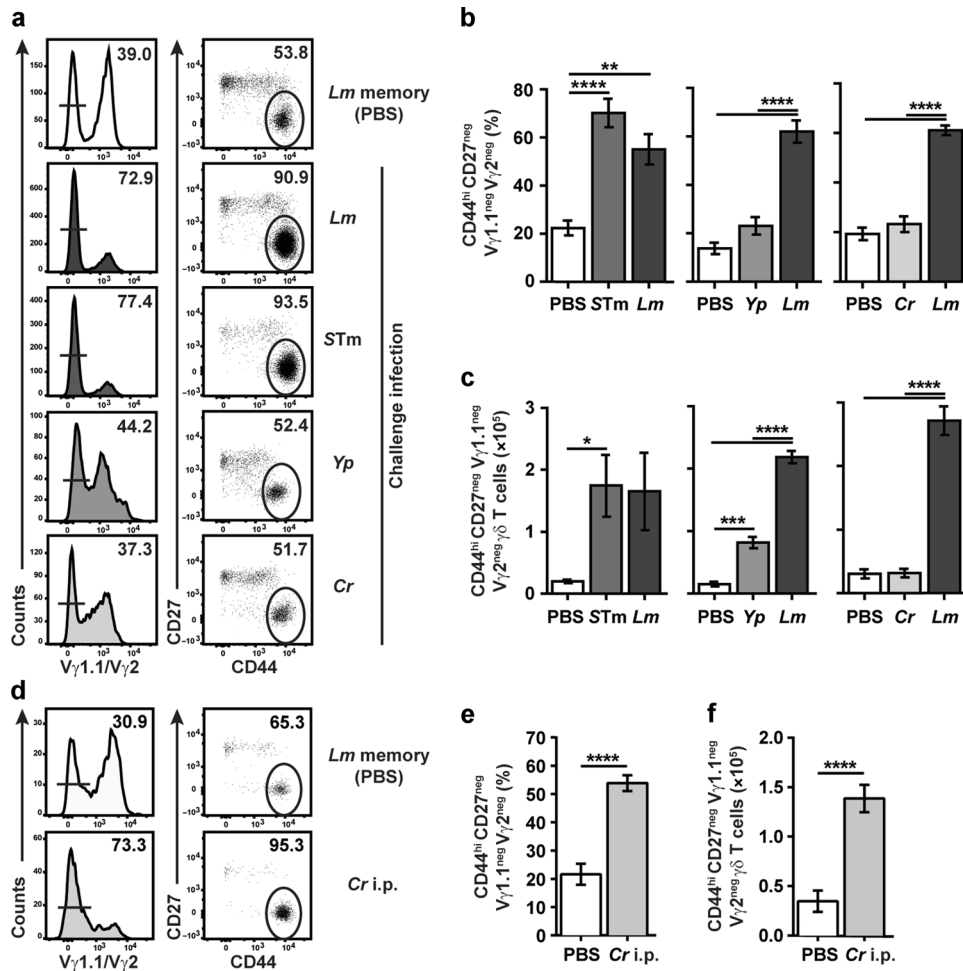


**Fig. 5 Differential response of memory  $\gamma\delta$  T cells to heterologous bacterial challenges in vivo.** **a–c** *Lm*-immune mice were left unchallenged (PBS) or challenged with the indicated bacteria.  $\gamma\delta$  T cells were analyzed in the MLN at 4 days post-recall (dpr) for STm and 5 dpi for *Yp*- and *Cr*-challenged mice. *Lm*-challenged mice were analyzed at the same time as the experimental group. **a** Representative flow plots are shown. Data represent the mean  $\pm$  SEM ( $n = 3–6$  mice/group) of the percentage of  $CD44^{hi} CD27^{neg} V\gamma 1.1^{neg} V\gamma 2^{neg}$  T cells among total  $\gamma\delta$  T cells (**b**) and their absolute numbers (**c**) and are representative of two independent experiments. **d–f** *Lm*-immune mice received PBS (Memory) or were i.p. challenged with *Cr*. After 5 days,  $\gamma\delta$  T cells were analyzed in the MLN. **d** Representative flow plots are shown. Data depict the mean  $\pm$  SEM ( $n = 3–5$  mice/group/experiment) of the percentage of  $CD44^{hi} CD27^{neg} V\gamma 1.1^{neg} V\gamma 2^{neg}$  T cells among total  $\gamma\delta$  T cells (**e**) and their absolute numbers (**f**) from the pool of two independent experiments. \* $p \leq 0.05$ ; \*\* $p \leq 0.01$ ; \*\*\* $p \leq 0.001$ ; \*\*\*\* $p \leq 0.0001$ .

### Adaptive $\gamma\delta$ T cells respond to diverse bacterial infections in vivo

As *Lm*-elicited memory  $V\gamma 4 V\delta 1$  T cells responded to diverse bacteria *ex vivo*, the response of *Lm*-elicited memory  $V\gamma 4 V\delta 1$  T cells to distinct foodborne pathogens was evaluated in vivo. First, a murine model of STm infection-induced colitis, which closely recapitulates human STm-induced gastroenteritis<sup>26,27</sup>, was used in *Lm*-immune mice<sup>28,29</sup>. A significant and robust expansion of  $CD44^{hi} CD27^{neg} V\gamma 1.1^{neg} V\gamma 2^{neg}$   $\gamma\delta$  T cells was observed that was remarkably similar to the recall response induced by *Lm* challenge (Fig. 5a–c). Foodborne infection of *Lm*-immune mice with the zoonotic pathogen *Yp*, which has a different life cycle and colonizes intestinal and extra-intestinal sites in both humans and mice<sup>30,31</sup>, induced a modest increase in the numbers of  $CD44^{hi} CD27^{neg} V\gamma 1.1^{neg} V\gamma 2^{neg}$   $\gamma\delta$  T cells (Fig. 5c). In contrast, foodborne infection of *Lm*-immune mice with *Cr*, a murine pathogen widely used to model human enteropathogenic and enterohaemorrhagic *E. coli* infection<sup>32</sup>, failed to induce a response of  $CD44^{hi} CD27^{neg} V\gamma 1.1^{neg} V\gamma 2^{neg}$   $\gamma\delta$  T cells in the MLN at 5 dpi (Fig. 5b, c). In contrast to the previously used pathogens which efficiently disseminate to the MLN, *Cr* is primarily confined to the lumen in immunocompetent hosts<sup>32,33</sup>. Since this spatial constraint may contribute to *Cr*'s inability to expand memory

$V\gamma 4 V\delta 1$  T cells in vivo, *Lm*-immune mice were i.p. infected with *Cr* to bypass the gut epithelium. This led to the early colonization of the MLN and spleen (Fig. S5) and robust response of  $CD44^{hi} CD27^{neg} V\gamma 1.1^{neg} V\gamma 2^{neg}$   $\gamma\delta$  T cells in the MLN at 5 dpi (Fig. 5d–f). Similar response patterns were observed after primary infection of naïve mice, as STm infection-induced colitis, i.p. *Cr* infection and, to a lesser extent, *Yp* infection elicited a  $CD44^{hi} CD27^{neg} V\gamma 1.1^{neg} V\gamma 2^{neg}$   $\gamma\delta$  T cell population, whereas foodborne *Cr* infection failed to do so (Fig. S6). Although the level of response varied between pathogens, these data demonstrate that intestinal adaptive  $V\gamma 4 V\delta 1$  T cells can respond to diverse bacterial pathogens with distinct replicative life cycles and suggest that the adaptive  $V\gamma 4 V\delta 1$  T cell response is a common feature of several bacterial pathogens. Taken together, these findings indicate the broadly reactive nature of adaptive  $V\gamma 4 V\delta 1$  T cells.

### *Lm*-elicited $\gamma\delta$ T cell recall responses to STm and i.p. *Cr* infections are mediated by the $\gamma\delta$ TCR

A key feature of memory T cells is their ability to respond efficiently upon antigen reencounter. Therefore, a side-by-side comparison of the  $CD44^{hi} CD27^{neg}$   $V\gamma 4$  T cell response to STm infection in naïve and *Lm*-immune mice was performed. STm

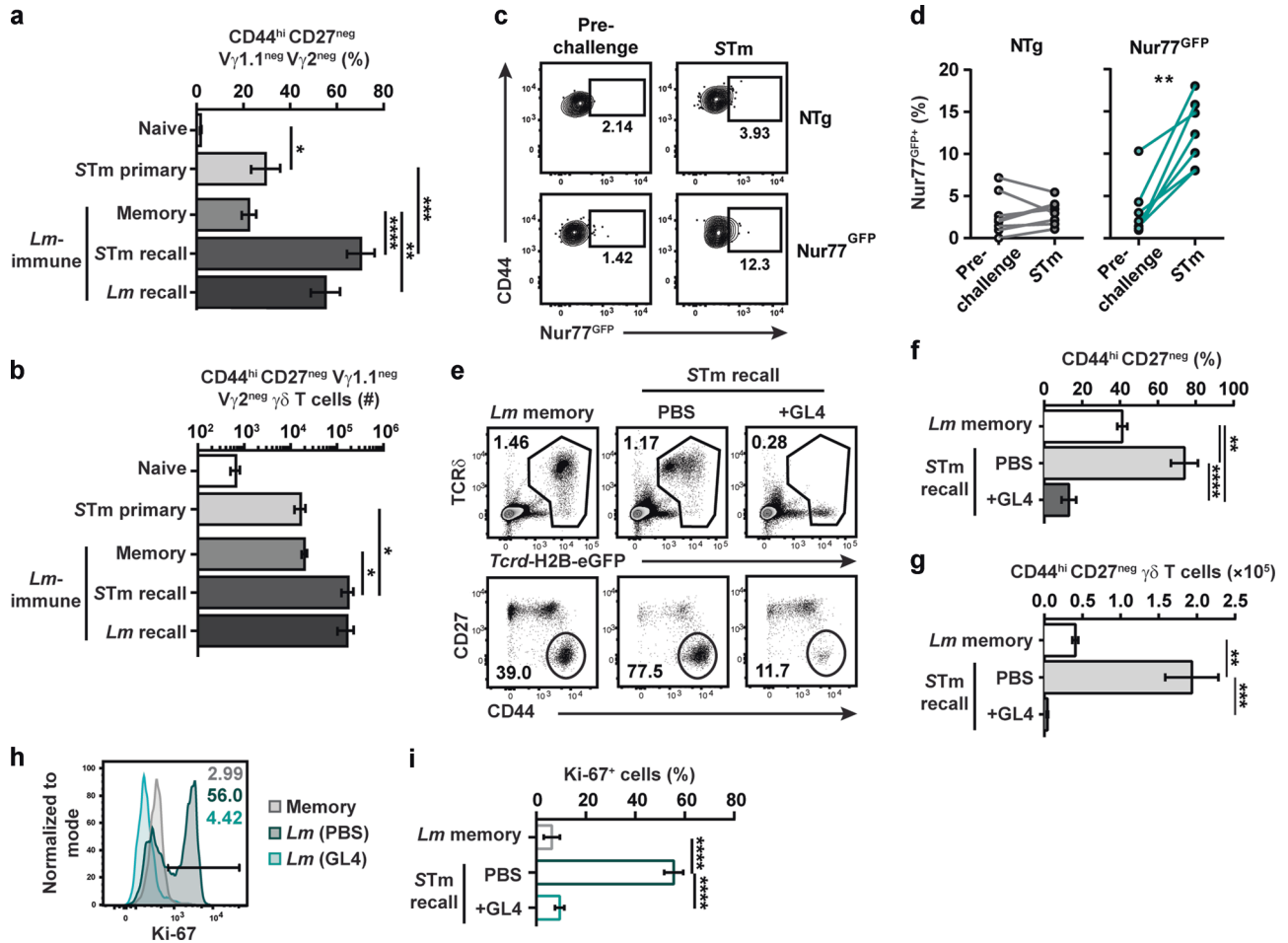


**Fig. 6** The  $\gamma\delta$ TCR critically regulates *Lm*-elicited  $\gamma\delta$  T cell recall-like response to STm infection. **a, b** *Lm*-immune mice received PBS (memory) or were challenged with either STm (STm recall) or *Lm* (*Lm* recall). Naïve mice were either given PBS (naïve) or infected with STm (STm primary). After 4 days,  $\gamma\delta$  T cells were analyzed in the MLN. Data show the mean  $\pm$  SEM ( $n = 3\text{--}6$  mice/group) of the percentage of CD44<sup>hi</sup> CD27<sup>neg</sup> V $\gamma$ 1.1<sup>neg</sup> V $\gamma$ 2<sup>neg</sup> T cells among total  $\gamma\delta$  T cells (**a**) and their absolute numbers (**b**) and are representative of two independent experiments. **c, d** GFP expression among circulating CD44<sup>hi</sup> CD27<sup>neg</sup> V $\gamma$ 1.1<sup>neg</sup> V $\gamma$ 2<sup>neg</sup>  $\gamma\delta$  T cells pre-challenge (25 to 31 days post-infection) and 4 days after STm challenge infection of *Lm*-immune Nur77<sup>GFP</sup> or non-transgenic (NTg) C57BL/6NJ mice. **c** Representative flow plots of GFP expression among CD44<sup>hi</sup> CD27<sup>neg</sup> V $\gamma$ 1.1<sup>neg</sup> V $\gamma$ 2<sup>neg</sup>  $\gamma\delta$  T cells are shown. **d** Cumulative data from two independent experiments ( $n = 2\text{--}5$  mice/group/experiment) are shown. Each line represents paired data from the same mouse pre- and post-challenge. **e–i** *Lm*-immune *Tcrd*-H2B-eGFP mice were treated with PBS or GL4 mAb and challenged with STm.  $\gamma\delta$  T cells (CD4<sup>neg</sup> CD8 $\alpha$ <sup>neg</sup> or TCR $\beta$ <sup>neg</sup> CD8 $\alpha$ <sup>neg</sup> GFP<sup>+</sup> single live lymphocytes) were analyzed in the MLN at 4 dpr. **e** Representative flow plots are shown. Cumulative data show the mean  $\pm$  SEM ( $n = 3\text{--}4$  mice/group/experiment) of the frequency of CD44<sup>hi</sup> CD27<sup>neg</sup>  $\gamma\delta$  T cells among total  $\gamma\delta$  T cells (**f**) and their absolute number (**g**) and depict two independent experiments. **h** Representative histograms of Ki-67 expression by CD44<sup>hi</sup> CD27<sup>neg</sup>  $\gamma\delta$  T cells are shown. **i** Graph shows the cumulative data of two independent experiments as the mean  $\pm$  SEM ( $n = 3$  mice/group/experiment) of Ki-67<sup>+</sup> cell frequency. \* $p \leq 0.05$ ; \*\* $p \leq 0.01$ ; \*\*\* $p \leq 0.001$ ; \*\*\*\* $p \leq 0.0001$ .

infection of *Lm*-immune mice elicited a robust response that was qualitatively similar to *Lm* recall infection (Fig. 6a, b). Additionally, STm infection of *Lm*-immune mice led to a significantly greater percentage and number of CD44<sup>hi</sup> CD27<sup>neg</sup> V $\gamma$ 1.1<sup>neg</sup> V $\gamma$ 2<sup>neg</sup>  $\gamma\delta$  T cells compared to STm infection of naïve mice (Fig. 6a, b). These data suggest that STm infection induces a recall response of *Lm*-elicited memory  $\gamma\delta$  T cells.

Given the critical role of the  $\gamma\delta$ TCR in mediating *Lm*-elicited memory  $\gamma\delta$  T cell recall response to *Lm* (Fig. 1), the importance of TCR signaling was assessed. Longitudinal analysis of circulating cells revealed a significant increase in the frequency of Nur77<sup>GFP</sup>-expressing CD44<sup>hi</sup> CD27<sup>neg</sup> V $\gamma$ 1.1<sup>neg</sup> V $\gamma$ 2<sup>neg</sup>  $\gamma\delta$  T cells 4 days after STm challenge infection (Fig. 6c, d). Furthermore, internalization of the  $\gamma\delta$ TCR in GL4-treated mice prevented CD44<sup>hi</sup> CD27<sup>neg</sup> V $\gamma$ 1.1<sup>neg</sup> V $\gamma$ 2<sup>neg</sup>  $\gamma\delta$  T cell expansion (Fig. 6e–g and S7a) and substantially reduced their proliferation (Fig. 6h, i) following STm challenge infection. However, GL4 treatment did not affect weight loss, fecal

shedding, or MLN STm burden (Fig. S7b–d). We previously showed that *Lm*-elicited  $\gamma\delta$  T cells provide protection against secondary *Lm* infection in concert with conventional T cells and that GL4 treatment alone does not affect *Lm* burden<sup>11</sup>. To determine whether TCR signaling contributes to the control of STm infection, we evaluated the effect of GL4 treatment on the ability of CD4- and CD8-depleted *Lm*-immune mice to control STm burden (Fig. S7e). Although STm burden in the MLN was similar between GL4- and PBS-treated mice, GL4 treatment resulted in a significant increase in STm burden in the spleen (Fig. S7f). These results reveal that the  $\gamma\delta$ TCR contributes to the optimal control of STm and suggest that STm-selected and cross-reactive  $\gamma\delta$  T cells can restrict STm dissemination to the spleen or mediate local antibacterial effects.

GL4 treatment also abrogated CD44<sup>hi</sup> CD27<sup>neg</sup> V $\gamma$ 1.1<sup>neg</sup> V $\gamma$ 2<sup>neg</sup>  $\gamma\delta$  T cell response to i.p. *Cr* infection without affecting weight loss (Fig. S8). Altogether, these data suggest that the  $\gamma\delta$ TCR is integral

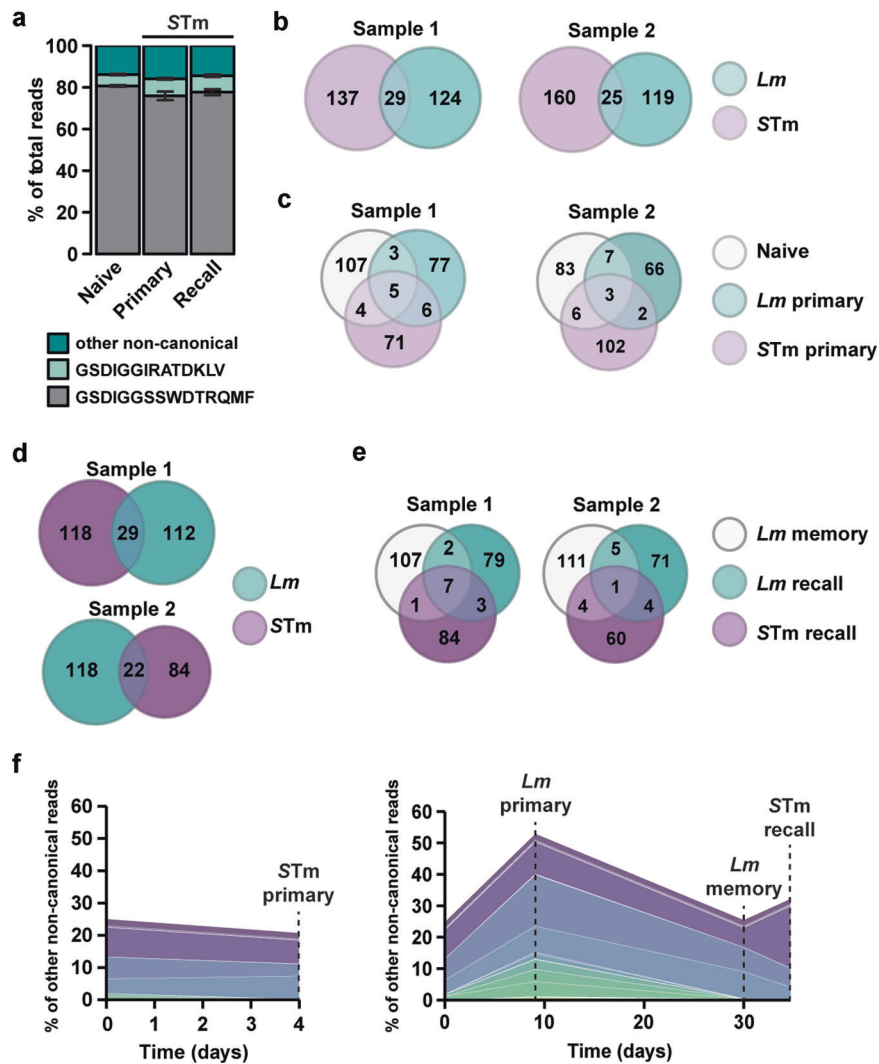


**Fig. 7** *Lm* and *STm*-colitis infections select for shared cross-reactive and distinct pathogen-specific non-canonical V $\delta$ 1 T clones in vivo. CD44<sup>hi</sup> CD27<sup>neg</sup> V $\gamma$ 1.1<sup>neg</sup> V $\gamma$ 2<sup>neg</sup>  $\gamma\delta$  T cells were sort-purified from the MLN during primary, memory, and recall responses to *Lm* infection, during primary and recall responses to *STm* infection, or from naïve Balb/c mice ( $n = 6$ –22 mice/group). CDR3 $\delta$  transcripts were sequenced and V $\delta$ 1 sequences were selected for further analyses. **a** Percent of total reads mapping to the canonical (gray), public non-canonical (light green), or other non-canonical sequences (dark green), in the naïve, *STm* primary, and *STm* recall samples averaged across two biological samples. **b** Venn diagrams show the number of expanded non-canonical clonotypes overlapping between primary *STm* and primary *Lm*. **c** Venn diagram shows the read frequency similarity of non-canonical clones present in naïve, *STm* primary, and *Lm* primary. Clonotypes with less than 25% difference between conditions are considered similar and shown as shared. **d**, **e** Similar analyses as in (**b**) and (**c**) were performed with *Lm* memory, *STm*-colitis challenge of *Lm*-immune mice, and *Lm* recall samples. **f** Clonotypes demonstrating a conventional memory response pattern to *Lm* (as identified in Fig. 2b) were analyzed for their primary and recall response to *STm*. Percent of non-canonical reads from two combined biological samples mapping to the selected sequences in naïve, *STm* primary, *Lm* primary, *Lm* memory, and *STm* recall samples.

to the recall response of *Lm*-elicited memory V $\gamma$ 4 V $\delta$ 1 T cells to heterologous infection and suggest that cells responding to *STm* in *Lm*-immune mice arise from the *Lm*-elicited memory pool.

#### **$\gamma\delta$ T cell responses to *Lm* and *STm* infections involve cross-reactive and non-overlapping pathogen-selected non-canonical clones**

Recognition of cognate antigen elicits robust T cell clonal expansion that leads to changes in clone abundance and alterations in TCR repertoire. To determine whether *Lm*-elicited memory V $\gamma$ 4 V $\delta$ 1 T cell clones respond to *STm*, the TCR $\delta$  repertoire of purified CD44<sup>hi</sup> CD27<sup>neg</sup> V $\gamma$ 4 T cells elicited by *STm* infection in naïve (*STm* primary) and *Lm*-immune mice (*STm* recall) were analyzed and compared to sorted *Lm*-elicited cells from age-matched mice (Fig. 2). The canonical and the public V $\delta$ 1 TCRs

represented the majority of (~85%) the repertoire of *STm* primary and *STm* recall samples, regardless of prior exposure to *Lm* (Fig. 7a). Interestingly, *STm* and *Lm* primary infections were selected for largely non-overlapping non-canonical clones (Fig. 7b). Only 29 and 25 overlapping clones were detected. The two infections also differentially affected the prevalence of overlapping non-canonical clones as the majority of the clonotypes analyzed showed a selective enrichment (>25% difference in read frequency) after either primary infection (Fig. 7c). Similar observations were made in *Lm*-immune mice infected with *Lm* or *STm* (Fig. 7d, e), suggesting that prior exposure to *Lm* does not impede the generation of subsequent non-canonical response to an unrelated pathogen. Overall, these results suggest that the non-canonical V $\gamma$ 4 V $\delta$ 1 repertoire is differentially shaped by unrelated infections, consistent with clonal selection mediated by distinct antigens.



Although these data suggest that the vast majority of infection-elicited non-canonical V $\gamma$ 4 V $\delta$ 1 T cell clones are specific to a given pathogen, the presence of conserved TCR sequences that expand after *Lm* and *STm* infections raised the question as to whether some clones could respond to both insults. To tackle this question, the response of the clones identified as *Lm*-selected clones in Fig. 2b was assessed after primary and recall *STm* infections. Out of 46 total sequences, 16 clones including one abundant clonotype (>4% of reads) expanded upon primary *STm* infection and 13 infrequent clones and 1 highly frequent clone (<0.5% and >6% of the reads, respectively) increased upon *STm* challenge of *Lm*-immune mice (Fig. 7f and Tables S1, S2). Among these clones, five infrequent clones expanded in response to both primary *STm* infection of naïve mice and challenge *STm* infection of *Lm*-immune mice. As such, ~9.2% of the non-canonical clones appeared cross-reactive and responded to both *Lm* and *STm* infections. Together, our findings reveal a complex heterogeneity of the memory V $\gamma$ 4 V $\delta$ 1 T cell population and demonstrate that the broad bacterial reactivity of adaptive V $\gamma$ 4 V $\delta$ 1 T cells results from a mixture of broadly reactive canonical and public TCRs, cross-reactive non-canonical TCRs, and pathogen-selected non-canonical TCRs.

## DISCUSSION

Here, a broad reactivity of the adaptive CD44<sup>hi</sup> CD27<sup>neg</sup> V $\gamma$ 4 V $\delta$ 1 T cell subset to gut disseminating pathogens was uncovered. This subset behaved like traditional adaptive T cells in their multifunctional response, the timing of accumulation in draining LN, and selection of non-canonical TCR elements. Unlike conventional memory cells, memory V $\gamma$ 4 V $\delta$ 1 T cells were broadly reactive to a wide array of pathogenic bacteria capable of extra-intestinal dissemination. TCR sequencing revealed that broad bacterial reactivity was largely due to the expansion of the canonical and public TCRs, with some contribution from cross-reactive non-canonical TCRs. Although V $\gamma$ 4 V $\delta$ 1 T cells are generally classified as innate-like<sup>34</sup>, TCR signaling was activated in adaptive  $\gamma\delta$  T cells upon exposure to different pathogenic bacteria and their responses were abrogated by anti-TCR $\delta$  treatment, providing strong evidence of the crucial role of the  $\gamma\delta$ TCR in regulating the recall response of memory V $\gamma$ 4 V $\delta$ 1 T cells. This suggests that antigen recognition or other TCR ligands are essential for their broad pathogen elicited response. While the V $\gamma$ 4 V $\delta$ 1 T cell response was broadly reactive to diverse pathogens at the population level, TCR sequencing revealed some level of pathogen specificity among a large subset of non-canonical TCRs. Thus, adaptive V $\gamma$ 4 V $\delta$ 1 T cells form a heterogeneous unconventional population that encompasses broadly reactive canonical and non-canonical clones, and pathogen-selected non-canonical clones which may function as gatekeepers against disseminating intestinal infections in the MLN.

Despite a uniform functional response of memory V $\gamma$ 4 V $\delta$ 1 T cells to all bacteria used in this study *ex vivo*, adaptive V $\gamma$ 4 V $\delta$ 1 T cells showed distinct response patterns to each pathogen *in vivo*. Both oral *STm* and foodborne *Yp* infection elicited an adaptive V $\gamma$ 4 V $\delta$ 1 T cell response, whereas foodborne *Cr* infection did not. A notable difference between these pathogens is their ability to efficiently disseminate extra-intestinally: while *STm* and *Yp* infection results in the colonization of the MLN<sup>28,31,35</sup>, *Cr* is less efficient at disseminating to the MLN after foodborne infection<sup>32</sup>. Bypassing the intestines by *i.p.* infection to allow *Cr* to colonize the MLN restored its ability to trigger a CD44<sup>hi</sup> CD27<sup>neg</sup> V $\gamma$ 1.1<sup>neg</sup> V $\gamma$ 2<sup>neg</sup>  $\gamma\delta$  T cell response. Although continuous sampling of the intestinal lumen by migratory DC is known to permit the dissemination of invasion defective bacteria to deeper tissues<sup>36</sup>, our observations suggest that factors besides colonization and DC migration are necessary to elicit an optimal proliferative response from adaptive V $\gamma$ 4 V $\delta$ 1 T cells. Because the  $\gamma\delta$ TCR mediates V $\gamma$ 4 V $\delta$ 1 T cell expansion and the ligand for the canonical V $\gamma$ 4 V $\delta$ 1 TCR is upregulated by infection<sup>20</sup>, high pathogen

burden or inflammation may be necessary to efficiently modulate the expression of canonical and non-canonical V $\gamma$ 4 V $\delta$ 1 T cells. Indeed, intestinal sampling only allows the uptake of a small number of bacteria<sup>36</sup>. Furthermore, we previously demonstrated that adaptive V $\gamma$ 4 V $\delta$ 1 T cells do not expand in response to invasive salmonellosis, a systemic typhoid-like disease in mice, which results in a lower organ burden than the *STm*-induced colitis model used in this study<sup>11,35</sup>. The inflammatory milieu may also regulate adaptive V $\gamma$ 4 V $\delta$ 1 T cell responses. Indeed, this study demonstrated that *Lm*-elicited memory CD44<sup>hi</sup> CD27<sup>neg</sup> V $\gamma$ 1.1<sup>neg</sup> V $\gamma$ 2<sup>neg</sup>  $\gamma\delta$  T cells expand in response to *STm*-induced colitis, whereas they fail to respond to invasive salmonellosis. Although these two models utilize the same pathogen, they elicit substantially different inflammatory responses<sup>28,29,35</sup>. While the typhoid model is characterized by diffuse enteritis and mononuclear immune infiltrate<sup>35</sup>, the *STm* infection-induced colitis leads to massive infiltration of neutrophils and inflammatory monocytes<sup>28,29</sup>. Thus, the respective contribution of inflammatory mediators and bacterial burden in the induction of adaptive V $\gamma$ 4 V $\delta$ 1 T cell responses needs further investigation.

In addition to regulating the generation and expansion of adaptive V $\gamma$ 4 V $\delta$ 1 T cells *in vivo*, all bacteria elicited a multifunctional response from *Lm*-elicited memory V $\gamma$ 4 V $\delta$ 1 T cells characterized by coproduction of IL-17A and IFN $\gamma$  *ex vivo*. As we previously showed that MHC-II<sup>+</sup> cells contribute to V $\gamma$ 4 V $\delta$ 1 T cell memory and recall effector functions<sup>11</sup>, bacterial pathogens may indirectly regulate  $\gamma\delta$  T cell function through DC activation and processes like antigen presentation or secretion of pro-inflammatory cytokines. Alternatively, adaptive V $\gamma$ 4 V $\delta$ 1 T cell responses may also be regulated by pattern recognition receptors (PRR). Indeed,  $\gamma\delta$  T cells themselves express PRR like NOD1, which has been associated with IFN $\gamma$  production in IL-17 producing  $\gamma\delta$  T cells<sup>37</sup>, and TLRs which can also mediate their functions even in the absence of TCR signaling<sup>5,6</sup>. These different but not mutually exclusive types of broad sensing modalities may contribute to the broad bacterial reactivity of memory V $\gamma$ 4 V $\delta$ 1 T cells.

Although V $\gamma$ 4 V $\delta$ 1 T cells are usually considered innate-like cells, TCR signaling was elicited after *Lm* and *STm* infection, and the  $\gamma\delta$ TCR was critical for the recall response of *Lm*-elicited  $\gamma\delta$  T cells to *Lm*, *STm* and *Cr* infection. Analysis of the CDR3 $\delta$  sequences suggests that cross-reactive and *STm*-selected non-canonical V $\delta$ 1 clones, in addition to broadly reactive canonical and public clones, account for the recall-like response to *STm* infection. This complexity is reminiscent of primate V $\delta$ 2<sup>+</sup> T cells, which can be divided into semi-invariant, innate-like V $\gamma$ 9<sup>+</sup> T cells that sense conserved antigens<sup>38,39</sup> and respond to both *Lm* and *STm*<sup>40,41</sup>, and adaptive V $\gamma$ 9<sup>-</sup> T cells that have a diverse TCR repertoire and clonally expand upon viral infection<sup>42</sup>. The TCR of the semi-invariant human circulating V $\gamma$ 9 V $\delta$ 2 and intestinal V $\gamma$ 4 T cell subsets can function as both an innate receptor that recognizes conserved molecules via its germline-encoded regions and a somatically rearranged receptor that confers restricted antigen specificity<sup>43,44</sup>. Our findings suggest that the adaptive V $\gamma$ 4 V $\delta$ 1 T cell response described here may also be mediated by two distinct antigen recognition modalities, with canonical and public V $\delta$ 1 clones recognizing conserved, host-derived antigens<sup>20</sup> while non-canonical clones are selected by infection-specific ligands.

An outstanding question raised by our observations relate to the respective contributions of canonical and non-canonical clones to the overall intestinal memory V $\gamma$ 4 V $\delta$ 1 T cell response. Innate-like V $\gamma$ 4 V $\delta$ 1 T cells are important producers of IL-17A in many contexts<sup>45</sup>, and contribute to IL-17A production after *i.p.* *Lm* infection<sup>46</sup>. Similarly, memory V $\gamma$ 4 V $\delta$ 1 T cells are the main source of IL-17A early after secondary exposure to *Lm*<sup>13</sup>. This suggests that canonical clones may be poised to rapidly produce large amounts of IL-17A. In contrast, the adaptive response pattern revealed by non-canonical clones and their TCR diversity suggests that these cells may be similar to conventional T cells and undergo analogous activation and differentiation steps. Although most IL-17A-producing  $\gamma\delta$  T cells develop before birth,

several studies demonstrated that de novo generation can occur in the periphery of adult mice upon inflammation<sup>47–49</sup>. Peripherally-induced  $\gamma\delta$  T cells showed some functional plasticity and were capable of coproducing IL-17A and IFN $\gamma$  in culture<sup>49</sup>. These observations suggest these cells could potentially tailor their effector functions to the pathogen encountered and the inflammatory environment they were activated in.

Collectively, the findings reported here reveal a striking heterogeneity of pathogen-reactive CD44<sup>hi</sup> CD27<sup>neg</sup> V $\gamma$ 4V $\delta$ 1 memory T cells, which mount robust TCR-mediated adaptive responses to disseminating bacterial pathogens owing to the concurrent involvement of broadly-reactive canonical and public TCRs and pathogen-selected non-canonical TCRs. These responses are reminiscent of the multifunctional adaptive-like V $\delta$ 2<sup>+</sup> T cell response reported in macaques immunized with an attenuated form of *Lm*<sup>40,50,51</sup>. As such, murine adaptive V $\gamma$ 4V $\delta$ 1 T cells share important features with primate V $\delta$ 2<sup>+</sup> T cells. Interestingly, *Lm*-elicited V $\delta$ 2<sup>+</sup> T cells were shown to provide protection to immunized macaques against heterologous infection<sup>40,50,51</sup>, which could have broad therapeutic implications. As our current understanding of how primate adaptive-like  $\gamma\delta$  T cells provide protection is limited, the mouse model of foodborne *Lm* infection provides an opportunity to gain insights into the mechanisms through which memory V $\gamma$ 4V $\delta$ 1 T cells mediate broad-spectrum immunity and to identify means to harness these unconventional cells for anti-infective therapy.

## METHODS

### Mice

All experiments were performed with female mice, with the exception of experiments performed in Nur77<sup>GFP</sup>, C57BL/6NJ (NTg) mice, and *Tcrd*-H2B-eGFP mice, which involved both males and females. Balb/c, Nur77<sup>GFP</sup>, and C57BL/6NJ mice were purchased from the Jackson Laboratory (Bar Harbor) and maintained under specific pathogen-free conditions. *Tcrd*-H2B-eGFP mice were kindly provided by Drs. Bernard Malissen and Immo Prinz, fully backcrossed onto a Balb/c background, and bred at Stony Brook University. Age-matched 9- to 12-week-old mice were used for all experiments. Nur77<sup>GFP</sup> and C57BL/6NJ mice were infected between 6 and 9 weeks old. Animals were randomly assigned to experimental groups. Males and females were equally distributed between groups to the best extent possible. All animal experiments were conducted in accordance with the Stony Brook University Institutional Animal Care and Use Committee and National Institutes of Health guidelines. Germ-free Balb/c mice were bred and maintained at the animal facility of Pohang University of Science and Technology (Pohang, Republic of Korea). All animal experiments were performed in accordance with institutional guidelines.

### Mouse infections and treatments

Unless otherwise specified, all mouse infections with *Lm*, *Yp*, and *Cr* were performed with foodborne infection as previously described<sup>11,13</sup>. Bacterial strains and infection doses are summarized in Table S3. GF and SPF control mice were infected by oral gavage with  $1 \times 10^8$  CFU InIA<sup>M</sup> *Lm*, strain 10403 s due to the increased susceptibility of GF mice to foodborne *Lm* infection. For STm infections, naive mice were left untreated or orally treated with 20 mg streptomycin solution in PBS 1 day prior to intragastric inoculation of STm. Systemic infection with *Cr* was performed through a single i.p. injection. When indicated, mice were given i.p. injections of 100  $\mu$ g anti-CD TCR (GL4 or UC7-13D5, Bio X Cell), 200  $\mu$ g anti-CD4 (GK1.5, Bio X Cell), or 500  $\mu$ g anti-CD8 $\alpha$  (2.43, Bio X Cell) antibody, alone or in combination, or PBS on days -3, -1, and +1 relative to recall infection.

### Isolation of leukocytes

MLN were harvested and mechanically dissociated into single-cell suspensions. Viable cells from single-cell suspensions were enumerated with the use of a Vi-CELL Viability Analyzer (Beckman Coulter). Cells were then directly stained or used for ex vivo stimulations.

### Antibodies and flow cytometry

For surface staining, cells were stained with the antibodies listed in Table S4, live/dead dye (Thermo Fisher Scientific), and anti-CD16/CD32 (Bio

X Cell). For detection of V $\gamma$ 4<sup>+</sup> cells, cells were first stained with 20  $\mu$ g of 1C10-1F7 antibody prior to secondary staining with a polyclonal rat anti-mouse IgG (Invitrogen). Cells were then stained with other antibodies. Intracellular cytokine staining was performed using BD Cytofix/Cytoperm Fixation/Permeabilization kit (BD Biosciences) according to the manufacturer's instructions. Ki-67 detection was performed using eBioscience Fc $\gamma$ 3/Transcription factor staining buffer set according to the manufacturer's instructions (Invitrogen). For the detection of pTyr319/Tyr352 Zap-70/Syk, cells were sequentially stained with Live/Dead dye, anti-CD3 $\epsilon$ , and anti-TCR $\delta$  antibodies, fixed with 4% paraformaldehyde containing 1.5% methanol, permeabilized using 100% ice-cold methanol and finally stained with the remaining antibodies. All samples were acquired on an LSRFortessa (BD Biosciences). Data were analyzed with FlowJo software (TreeStar).

### Heat-killed bacteria preparation

Heat-killed bacteria were produced by incubating log-phase growing bacteria resuspended in PBS at 56 °C for 4 h. Killing efficiency was assessed by plating undiluted bacteria on appropriate agar plates. The absence of the colony was confirmed 24–48 h later.

### Ex vivo stimulations

Single MLN cell suspensions from *Lm*-immune mice were adjusted to a concentration of  $5 \times 10^5$  cells/ml in IMDM media containing 10% FBS, 10 mM HEPES, 1 mM sodium pyruvate, 2 mM GlutaMAX<sup>TM</sup> supplement, and 1X MEM nonessential amino acids solution, all from Thermo Fisher Scientific. Cells were cultured at 37 °C, 5% CO<sub>2</sub> for the incubation period indicated in the figures. All HK bacteria were added at an MOI of 10. Anti-CD3 $\epsilon$  was used at 10  $\mu$ g/ml, and plates were coated in PBS overnight the day prior to the stimulation. Anti-CD28 antibody was used at 2  $\mu$ g/ml and added to the culture. GL4 antibody was either used at 1 or 10  $\mu$ g/ml as indicated, and plates were coated in PBS overnight the day prior to the stimulation. Antibody-mediated stimulations were performed for 6 h. Intracellular protein transport was blocked by the addition of BD GolgiPlug<sup>TM</sup> (BD Biosciences) 5 to 6 h prior to the end of the stimulation.

### CDR3 $\delta$ and CDR3 $\gamma$ sequencing

Single-cell suspensions from MLN ( $n = 6–22$  mice/group) were generated as described before from *Lm*-infected mice at 9 (primary) and 37 (memory) dpi and 5 days after *Lm* recall infection. Harvest was performed 4 dpi for STm infected mice (primary infection and recall infection of *Lm*-immune mice). Naïve cells were isolated from MLN, spleen, and pLN (inguinal, brachial, axillary, and cervical).  $\gamma\delta$  T cells were enriched by negative selection using B220-, CD8 $\alpha$ -, and CD4-biotin antibodies and MagniSort Streptavidin Negative Selection Beads (Invitrogen). The enriched fraction was then used to sort single live CD44<sup>hi</sup> CD27<sup>neg</sup> V $\gamma$ 4 T cells on a FACS Aria IIIu (BD) (sorting strategy showed in Fig. S3). RNA was extracted using RNeasy Mini Kit (Qiagen) according to the manufacturer's instructions. Library amplification and sequencing using Illumina MiSeq (CDR3 $\delta$ ) and Illumina MiSeq Nano (CDR3 $\gamma$ ) were performed by iRepertoire Inc. (Huntsville).

### CDR3 $\delta$ sequencing post-analysis

CDR3 clonotypes expressing mTRDV4 in the V region were selected for analysis. mTRDV4 sequences represented 96.04 to 99.89% of the total TCR $\delta$  reads analyzed. The canonical GSDIGGSSWDTRQMF and public GSDIGGIR-ATDKLV sequences were excluded from the detailed analysis, except in Figs. 2a and 7a. Non-canonical clonotypes in Fig. 2b were selected by determining which clonotypes with non-zero reads in the naive sample had a greater number of reads upon primary infection with *Lm*, and a greater number of reads at *Lm* recall relative to memory. The frequency of the selected CDR3 clonotypes were subsequently analyzed in STm primary and STm recall samples as shown in Fig. 7f. Venn diagrams in Fig. 7b, d show the repertoire overlap between the non-canonical sequences expanded in *Lm* (read counts *Lm* primary > Naïve) and STm primary (read counts STm-colitis > Naïve) or *Lm* and STm recall vs memory samples, respectively. Venn diagrams based on read frequency similarity (Fig. 7c, e) use a 25% threshold calculated using the absolute difference of the percent of total non-canonical reads per compared sample. Clonotypes with percent of non-canonical reads less than 0.01% were excluded to avoid comparing non-existent sequences.

### CDR3 $\gamma$ sequencing post-analysis

Basic analysis of the CDR3 $\gamma$  clonotype representation in each sample was provided by iRepertoire Inc. (Huntsville). Segment usage was represented using GraphPad Prism 6 software (La Jolla, CA).

### STm fecal shedding and organ burden

Fecal pellets were collected, weighed, and diluted in PBS. MLN were collected at day 4 and mechanically dissociated through a 70  $\mu$ m filter. Serial dilutions were prepared in DPBS and plated onto lysogeny agar plates supplemented with 50  $\mu$ g/ml nalidixic acid.

### Statistics

Statistical analyses were performed in GraphPad Prism software (La Jolla, CA). Ordinary one-way ANOVA with the Tukey multiple comparison test was used for comparison of more than two unpaired groups and two-way ANOVA with the Tukey multiple comparison test for longitudinal group comparisons. Comparison of Nur77<sup>GFP</sup> expression in the blood between memory and recall time points were performed using Paired Student *t*-test. Differences in pZap-70/Syk expression were determined using paired one-way ANOVA with the Tukey multiple comparison test. Unpaired Student *t*-test was used otherwise. Differences are represented as follow: \**p*  $\leq$  0.05; \*\**p*  $\leq$  0.01; \*\*\**p*  $\leq$  0.001; \*\*\*\**p*  $\leq$  0.0001.

### DATA AVAILABILITY

The datasets generated during this study are available at the SRA database, under the BioProject accession number PRJNA684361. The codes generated during this study are available upon request.

### REFERENCES

- Garrett, W. S., Gordon, J. I. & Glimcher, L. H. Homeostasis and inflammation in the intestine. *Cell* **140**, 859–870 (2010).
- Hooper, L. V. & Macpherson, A. J. Immune adaptations that maintain homeostasis with the intestinal microbiota. *Nat. Rev. Immunol.* **10**, 159–169 (2010).
- Nielsen, M. M., Witherden, D. A. & Havran, W. L. Gammadelta T cells in homeostasis and host defence of epithelial barrier tissues. *Nat. Rev. Immunol.* **17**, 733–745 (2017).
- Havran, W. L., Chien, Y. H. & Allison, J. P. Recognition of self antigens by skin-derived T cells with invariant gamma delta antigen receptors. *Science* **252**, 1430–1432 (1991).
- Sutton, C. E. et al. Interleukin-1 and IL-23 induce innate IL-17 production from gammadelta T cells, amplifying Th17 responses and autoimmunity. *Immunity* **31**, 331–341 (2009).
- Martin, B., Hirota, K., Cua, D. J., Stockinger, B. & Veldhoen, M. Interleukin-17-producing gammadelta T cells selectively expand in response to pathogen products and environmental signals. *Immunity* **31**, 321–330 (2009).
- Tan, L. et al. A fetal wave of human type 3 effector gammadelta cells with restricted TCR diversity persists into adulthood. *Sci Immunol.* **6**, eabf0125 (2021).
- Netea, M. G., Latz, E., Mills, K. H. & O'Neill, L. A. Innate immune memory: a paradigm shift in understanding host defense. *Nat. Immunol.* **16**, 675–679 (2015).
- Khairallah, C., Chu, T. H. & Sheridan, B. S. Tissue adaptations of memory and tissue-resident gamma delta T cells. *Front. Immunol.* **9**, 2636 (2018).
- Wollert, T. et al. Extending the host range of *Listeria monocytogenes* by rational protein design. *Cell* **129**, 891–902 (2007).
- Sheridan, B. S. et al. Gammadelta T cells exhibit multifunctional and protective memory in intestinal tissues. *Immunity* **39**, 184–195 (2013).
- Garman, R. D., Doherty, P. J. & Raulet, D. H. Diversity, rearrangement, and expression of murine T cell gamma genes. *Cell* **45**, 733–742 (1986).
- Romagnoli, P. A., Sheridan, B. S., Pham, Q. M., Lefrancois, L. & Khanna, K. M. IL-17A-producing resident memory gammadelta T cells orchestrate the innate immune response to secondary oral *Listeria monocytogenes* infection. *Proc. Natl Acad. Sci. USA* **113**, 8502–8507 (2016).
- Murphy, A. G. et al. *Staphylococcus aureus* infection of mice expands a population of memory gammadelta T cells that are protective against subsequent infection. *J. Immunol.* **192**, 3697–3708 (2014).
- Misiak, A., Wilk, M. M., Raverdeau, M. & Mills, K. H. IL-17-producing innate and pathogen-specific tissue resident memory gammadelta T cells expand in the lungs of *Bordetella pertussis*-infected mice. *J. Immunol.* **198**, 363–374 (2017).
- Dillen, C. A. et al. Clonally expanded gammadelta T cells protect against *Staphylococcus aureus* skin reinfection. *J. Clin. Invest.* **128**, 1026–1042 (2018).
- Hartwig, T., Pantelyushin, S., Croxford, A. L., Kulig, P. & Becher, B. Dermal IL-17-producing gammadelta T cells establish long-lived memory in the skin. *Eur. J. Immunol.* **45**, 3022–3033 (2015).
- Ramirez-Valle, F., Gray, E. E. & Cyster, J. G. Inflammation induces dermal Vgamma4+ gammadeltaT17 memory-like cells that travel to distant skin and accelerate secondary IL-17-driven responses. *Proc. Natl Acad. Sci. USA* **112**, 8046–8051 (2015).
- Chien, Y. H., Meyer, C. & Bonneville, M. Gammadelta T cells: first line of defense and beyond. *Annu. Rev. Immunol.* **32**, 121–155 (2014).
- Aydintug, M. K., Roark, C. L., Chain, J. L., Born, W. K. & O'Brien, R. L. Macrophages express multiple ligands for gammadelta TCRs. *Mol. Immunol.* **45**, 3253–3263 (2008).
- Moran, A. E. et al. T cell receptor signal strength in Treg and iNKT cell development demonstrated by a novel fluorescent reporter mouse. *J. Exp. Med.* **208**, 1279–1289 (2011).
- Koenecke, C. et al. In vivo application of mAb directed against the gammadelta TCR does not deplete but generates “invisible” gammadelta T cells. *Eur. J. Immunol.* **39**, 372–379 (2009).
- Hatano, S. et al. Development of a new monoclonal antibody specific to mouse Vgamma6 chain. *Life Sci. Alliance* **2**, e201900363 (2019).
- Hand, T. W. et al. Acute gastrointestinal infection induces long-lived microbiota-specific T cell responses. *Science* **337**, 1553–1556 (2012).
- Duan, J., Chung, H., Troy, E. & Kasper, D. L. Microbial colonization drives expansion of IL-1 receptor 1-expressing and IL-17-producing gamma/delta T cells. *Cell Host Microbe* **7**, 140–150 (2010).
- Zhang, S. et al. Molecular pathogenesis of *Salmonella enterica* serotype typhimurium-induced diarrhea. *Infect. Immun.* **71**, 1–12 (2003).
- Rabsch, W., Tschape, H. & Bauml, A. J. Non-typhoidal salmonellosis: emerging problems. *Microbes Infect.* **3**, 237–247 (2001).
- Barthel, M. et al. Pretreatment of mice with streptomycin provides a *Salmonella enterica* serovar Typhimurium colitis model that allows analysis of both pathogen and host. *Infect. Immun.* **71**, 2839–2858 (2003).
- McLaughlin, P. A. et al. Inflammatory monocytes provide a niche for *Salmonella* expansion in the lumen of the inflamed intestine. *PLoS Pathog.* **15**, e1007847 (2019).
- Davis, K. M. All *Yersinia* are not created equal: phenotypic adaptation to distinct niches within mammalian tissues. *Front. Cell Infect. Microbiol.* **8**, 261 (2018).
- Zhang, Y., Khairallah, C., Sheridan, B. S., van der Velden, A. W. M. & Bliska, J. B. CCR2(+) inflammatory monocytes are recruited to *Yersinia pseudotuberculosis* pyogranulomas and dictate adaptive responses at the expense of innate immunity during oral infection. *Infect. Immun.* **86**, e00782-17 (2018).
- Collins, J. W. et al. *Citrobacter rodentium*: infection, inflammation and the microbiota. *Nat. Rev. Microbiol.* **12**, 612–623 (2014).
- Vallance, B. A., Deng, W., Jacobson, K. & Finlay, B. B. Host susceptibility to the attaching and effacing bacterial pathogen *Citrobacter rodentium*. *Infect. Immun.* **71**, 3443–3453 (2003).
- Chien, Y. H., Zeng, X. & Prinz, I. The natural and the inducible: interleukin (IL)-17-producing gammadelta T cells. *Trends Immunol.* **34**, 151–154 (2013).
- Santos, R. L. et al. Animal models of *Salmonella* infections: enteritis versus typhoid fever. *Microbes Infect.* **3**, 1335–1344 (2001).
- Rescigno, M. et al. Dendritic cells express tight junction proteins and penetrate gut epithelial monolayers to sample bacteria. *Nat. Immunol.* **2**, 361–367 (2001).
- Schmolka, N. et al. MicroRNA-146a controls functional plasticity in gammadelta T cells by targeting NOD1. *Sci Immunol.* **3**, eaao1392 (2018).
- Vantourout, P. et al. Heteromeric interactions regulate butyrophilin (BTN) and BTN-like molecules governing gammadelta T cell biology. *Proc. Natl Acad. Sci. USA* **115**, 1039–1044 (2018).
- Rigau, M. et al. Butyrophilin 2A1 is essential for phosphoantigen reactivity by gammadelta T cells. *Science* **367**, eaay5516 (2020).
- Ryan-Payseur, B. et al. Multieffector-functional immune responses of HMBPP-specific Vgamma2Vdelta2 T cells in nonhuman primates inoculated with *Listeria monocytogenes* DeltaactA prfA\*. *J. Immunol.* **189**, 1285–1293 (2012).
- Hara, T. et al. Predominant activation and expansion of V gamma 9-bearing gamma delta T cells in vivo as well as in vitro in *Salmonella* infection. *J. Clin. Invest.* **90**, 204–210 (1992).
- Davey, M. S. et al. The human Vdelta2(+) T-cell compartment comprises distinct innate-like Vgamma9(+) and adaptive Vgamma9(-) subsets. *Nat. Commun.* **9**, 1760 (2018).
- Melandri, D. et al. The gammadeltaTCR combines innate immunity with adaptive immunity by utilizing spatially distinct regions for agonist selection and antigen responsiveness. *Nat. Immunol.* **19**, 1352–1365 (2018).
- Willcox, C. R. et al. Butyrophilin-like 3 directly binds a human Vgamma4(+) T cell receptor using a modality distinct from clonally-restricted antigen. *Immunity* **51**, 813–825 (2019).
- McKenzie, D. R., Comerford, I., Silva-Santos, B. & McColl, S. R. The emerging complexity of gammadeltaT17 Cells. *Front. Immunol.* **9**, 796 (2018).

46. Hamada, S. et al. IL-17A produced by gammadelta T cells plays a critical role in innate immunity against listeria monocytogenes infection in the liver. *J. Immunol.* **181**, 3456–3463 (2008).
47. Zeng, X. et al. gammadelta T cells recognize a microbial encoded B cell antigen to initiate a rapid antigen-specific interleukin-17 response. *Immunity* **37**, 524–534 (2012).
48. Papotto, P. H. et al. IL-23 drives differentiation of peripheral gammadelta17 T cells from adult bone marrow-derived precursors. *EMBO Rep.* **18**, 1957–1967 (2017).
49. Muschaweckh, A., Petermann, F. & Korn, T. IL-1beta and IL-23 promote extrathymic commitment of CD27+CD122- gammadelta T cells to gammadeltaT17 cells. *J. Immunol.* **99**, 2668–2679 (2017).
50. Frencher, J. T. et al. HMBPP-deficient Listeria mutant immunization alters pulmonary/systemic responses, effector functions, and memory polarization of Vgamma2Vdelta2 T cells. *J. Leukoc. Biol.* **96**, 957–967 (2014).
51. Shen, L. et al. Immunization of Vgamma2Vdelta2 T cells programs sustained effector memory responses that control tuberculosis in nonhuman primates. *Proc. Natl Acad. Sci. USA* **116**, 6371–6378 (2019).

## ACKNOWLEDGEMENTS

This work is supported by NIH grants R01-AI076457 (B.S.S.), R01-AI099222 (J.B.B.), R01-AI101221 (A.W.M.v.V.), K12-GM102778 (Z.Q.), T32-AI007539 (J.N.I. and T.H.C.), and P01-AI056172 (L.P.), a Mathers Charitable Foundation grant MF-1901-00210 (B.S.S.), project IBS-R005-D1 (K.S.K.) from the Institute for Basic Science, National Research Foundation, Korean Ministry of Science, Information/Communication Technology and Future Planning, and funds provided by The Research Foundation of New York and Stony Brook University. We thank Dr. Pablo Romagnoli for advice and discussion on the manuscript.

## AUTHOR CONTRIBUTIONS

C.K. and B.S.S. designed the research. A.W.M.v.V. and J.B.B. consulted with *STm*-colitis and *Yp*, respectively. C.K., J.A.B., Z.Q., Y.Z., T.H.C., J.N.I., and G.R. performed the experiments in SPF mice. K.C., K.S.K., and C.D.S. performed and supervised the experiments in GF mice. S.H. and Y.Y. provided the 1C10-1F7 antibody and consulted on the staining. C.K. and O.G. analyzed the data. C.K. and B.S.S. interpreted the data. C.K. wrote the manuscript. B.S.S. and C.K. edited the manuscript.

## COMPETING INTERESTS

The authors declare no competing interests.

## ADDITIONAL INFORMATION

**Supplementary information** The online version contains supplementary material available at <https://doi.org/10.1038/s41385-021-00447-x>.

**Correspondence** and requests for materials should be addressed to B.S.S.

**Reprints and permission information** is available at <http://www.nature.com/reprints>

**Publisher's note** Springer Nature remains neutral with regard to jurisdictional claims in published maps and institutional affiliations.